DOI: 10.1002/chem.200902764

Control of Relative Direction and Amplitude in Extension/Contraction Motions of Molecular Strands Induced by Ion Binding

Adrian-Mihail Stadler,[a, b] Juan Ramírez,[a, c] and Jean-Marie Lehn*[a]

Abstract: The shape of ligand strands composed of six-membered aza-heterocycles (het) connected at the α and α′ positions by hydrazone (hyz) units is determined in a predictable fashion by the nature of the heterocyclic groups (pyridine, pyrimidine, pyrazine etc.), and covers the range from extended linear to compact helical structures. The binding of metal ions to the coordination subunits, defined by the het-hyz sequences, leads to marked shape changes by inter-converting bent and linear conformations of the subunits, thus inducing relative motions of strand domains either in the same (*con*-sense, "twirling") or in opposite (*dis*-sense, "flapping") directions. The amplitude of the motion induced by metal-ion binding and release and the relative directions of the formal motions can be controlled by the nature of the heterocyclic units. Thus, motions around a central 4,6-disubstituted pyrimidine are *dis*-sense motions, whereas there are *con*-sense motions around a central 2,5-disubstituted pyrazine unit, as illustrated by model ligands **1** and **2**, respectively. The more extended helical **3** and undulating (zigzag shape) **4** ligands undergo larger-amplitude motions combining the relative displacements displayed by **1** and **2**. Ligands **3** and **4** form linear tetranuclear Pb^{II} and Zn^{II} complexes, thus producing an extension motion. The same holds for $[Ru(\mathbf{4})(terpy)_4](PF_6)_8$ (terpy = terpyridine). Reversible acid–base-triggered molecular motions have been generated with $[Zn_4(\mathbf{4})(OTf)_8]$ (TfOH = triflic acid).

Keywords: molecular devices · molecular motion · nitrogen heterocycles · N ligands · structural codons

Introduction

Molecular strands undergo intramolecular self-organisation into specific architectures as a result of the conformational features of their components and the non-bonding intramolecular interactions between them. They may present a full range of folded structures from compact helices to extended linear arrangements. Such structures play a crucial role in particular in bio-macromolecules, as in the α-helix or β-sheet domains in proteins,[1] the double helix of DNA or the overall shape of viral coat proteins.

The design of non-biological entities that spontaneously organise into well-defined architectures is of great significance both for the understanding of the basic features that also determine biological structures, and for the potential applications in materials science, in particular nanodevice technology. It requires the identification of structural codons,[2–4] structural motifs that enforce the shape of molecular strands. Folding[5] is a particularly interesting structural characteristic. Thus, helical shapes may be induced in synthetic entities by hydrogen bonding,[6] conformational properties,[3] medium effects[7] etc.

In our laboratory, we have in particular demonstrated that specific sequences of connected aza-heterocyclic groups may be considered as helicity codons or linearity codons, which enforce respectively helical or linear shapes or intermediate, zigzag-type, undulating ones. Thus, pyridine–pyrimidine (py-pym) sequences (py = 2,6-disubstituted pyridine, pym = 4,6-disubstituted pyrimidine) yield multi-turn helices,[4] whereas py-py ones give linear strands.[8] The origin of these structure-enforcing features lies in the strong prefer-

[a] Dr. A.-M. Stadler, Dr. J. Ramírez, Prof. Dr. J.-M. Lehn
Laboratoire de Chimie Supramoléculaire
Institut de Science et d'Ingénierie Supramoléculaires
Université de Strasbourg
8 Allée Gaspard Monge, Strasbourg 67083 (France)
Fax: (+33) 368-855-140
E-mail: lehn@isis.u-strasbg.fr

[b] Dr. A.-M. Stadler
Karlsruhe Institute of Technology (KIT)
Forschungszentrum Karlsruhe (FZK)
Institute for Nanotechnology (INT)
Postfach 3640, 76021 Karlsruhe (Germany)

[c] Dr. J. Ramírez
Present address:
IGBMC Biomolecular NMR Group, CNRS UMR 7104
Rue Laurent Fries, 67400 Illkirch (France)

ence of α,α′-connected aza-heterocycles[9] for the *transoid* over *cisoid* orientation by about 25–30 kJ mol^{-1} (Scheme 1 a).[9]

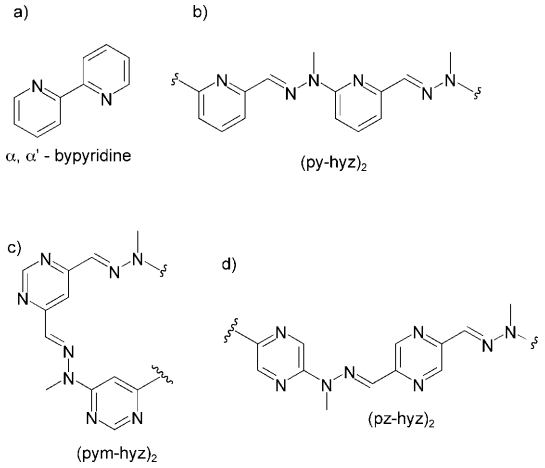

Scheme 1. *Transoid* conformation of α,α′-bipyridine (a) and examples (b–d) of sequences (het-hyz)$_2$ containing het-hyz codons.

It was also shown that the py group could be replaced by the isosteric but synthetically much more favourable hydrazone (hyz) unit[10] with conservation of the coding features. The influence of the nature of the heterocycle (het) on the global shape of the ligand of general formula py$_1$-(hyz-het)$_n$-hyz-py$_1$ (py$_1$ = 2-substituted pyridine) may be analysed as follows: het = py → linear shape (Scheme 1 b), het = pym → bent shape (Scheme 1 c) or helical shape (for larger strands), and het = pz → linear shape (pz = pyrazine; Scheme 1 d). The sequence het-hyz (Scheme 1 b–d) can be defined as a structural (geometry) codon, the unit containing the geometrical information that directs the shape of the molecule.

A further highly significant factor consists in the ability of such oligoheterocyclic strands to switch between defined (helical or linear) shapes by interaction with metal ions, which convert the *transoid* orientations to the *cisoid* ones on coordination. The α,α′-interconnected sequence het-hyz-het acts as a terpyridine (terpy)-like ligand and may coordinate a metal ion such as Zn^{II} or Pb^{II} (Scheme 2). This coordination process results in a change of the conformation from all-*transoid* to all-*cisoid* and therefore in the relative orientation of the het groups. Thus, the inter-conversion between helical and linear entities was achieved, which generated reversible molecular motions of large amplitude from a helical strand to a linear one in the complex[11] or, conversely, from a linear ligand to a helical complex.[12]

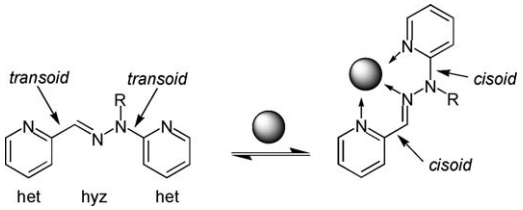

Scheme 2. Conformational change on coordination of a metal ion to a terpyridine-like het-hyz-het sequence.

The choice and combination of different types of heterocycles define the geometry of the ligand strand before and after interaction with the metal ion. Thus, the selection of the nature and sequence of heterocyclic units provides the means to control the geometry of the ligand and, further, to conceive and synthesise various strands with the aim of controlling the type and amplitude of the molecular motions generated upon metal-ion coordination.

Dependence of relative molecular motions on strand constitution: The type of molecular motion resulting from the change in ligand geometry on coordination of metal ions depends on the nature of the six-membered heterocycles incorporated (Scheme 3). The sequence pym$_1$-hyz-pym$_2$-hyz-pym$_3$, which presents a central pym unit, has a plane of symmetry perpendicular to the pym$_2$ group that is conserved on cation coordination. Therefore, the relative displacement of the ligand branches with respect to pym occurs in the opposite direction (*dis*-sense; Scheme 3 a). On the other hand, the ligand sequence pz$_1$-hyz-pz$_2$-hyz-pz$_3$ containing a central pz unit has a centre of symmetry (inversion centre) that is conserved on coordination, which implies that the ligand branches connected to the pz ring undergo a relative displacement in the same direction (*con*-sense; Scheme 3 b).

The relative motions of the heterocyclic branches with respect to the central core heterocyclic group can be represented schematically by considering the centres of the three heterocycles from the above sequences. The angle formed by the centres of the heterocycles pym$_1$, pym$_2$ and pym$_3$ is

Abstract in French: *La forme des brins constitués d'hétérocycles azotés à six chaînons (het), connectés en positions α et α′ par des unités hydrazone (hyz), est déterminée de manière prédictible par la nature des hétérocycles (pyridine, pyrimidine, pyrazine etc.). L'interaction des cations métalliques appropriés avec les sous-unités het-hyz, engendre l'inter-conversion des conformations linéaire et coudée des sous-unités, induisant ainsi des mouvements relatives des domaines du ligand dans le même sens (*con*-sens ou "tournoiement") ou dans le sens opposé (*dis*-sens ou "battement"). L'amplitude et les directions relatives du mouvement peuvent être contrôlées par le biais de la nature des unités hétérocycliques. L'unité pyrimidine 4,6-disubstituée induit des mouvements de battement, alors que la pyrazine 2,5-disubstituée induit des mouvements de tournoiement. Le ligand hélicoïdal **3** et le ligand en forme de zigzag **4** subissent d'importants changements d'amplitude lors de la formation de leurs complexes tétranucléaires de Pb^{II} ou Zn^{II}. Ces réactions ont été intégrées dans des systèmes de mouvements moléculaires modulés par des ajouts alternatifs d'acide et de base.*

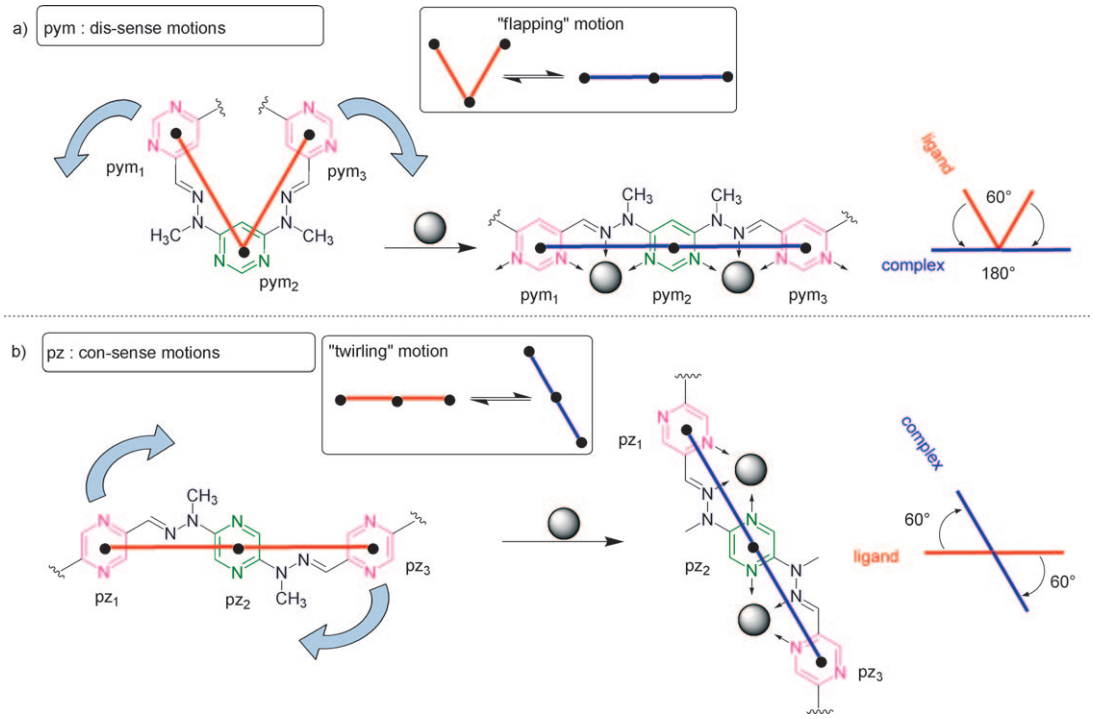

Scheme 3. *Dis*- (a) and *con*-sense (b) in-plane displacements induced by cation coordination to two sequences containing as central ring either a pyrimidine (a) or a pyrazine (b) group.

60° in the free ligand and is transformed in a 180° angle on coordination, by bending in opposite directions. The angle formed by the centres of the heterocycles pz_1, pz_2 and pz_3 is 180° in the free ligand and is transformed by coordination into a new 180° angle, rotated by 60° through motion of the branches in the same direction. The ditopic ligands **1** and **2** (Scheme 4) may be considered as models of these two types, respectively (Scheme 3a and b).

The consequence at the molecular scale of the coordination of the appropriate cation is, for pym-hyz-based strands, an unfolding (from a bent or helical shape into a linear shape), whereas for pz-hyz-based strands there is conservation of the global shape (from a linear ligand to a linear alternate up-and-down array of metal ions). Thus, the replacement of pym units by pz units in a given strand introduces in the free ligand as well as in its complexes both novel structural and functional features, and generates complexes with alternating cation positioning[13] and with extended conjugation properties.[14]

The control of the structural and functional features of strands, able to generate metallo-supramolecular architectures, by the nature of the key heterocycles is nowadays a challenging domain. For example, from a structural point of view, the control of molecular architecture was achieved by use of the appropriate ligand isomer, which resulted in a mononuclear Co^{III} corner-type complex when the central unit was a 2,3-disubstituted pyrazine, whereas a tetranuclear [2×2] grid-type Co^{III} complex was formed when it was a 2,5-disubstituted pyrazine.[15] From a functional point of view, it was possible to control the dimensions of the internal cavity of Cu^{I} [2×2] grid-type complexes, and consequently the capacity to encapsulate anions, by choosing as central unit either a 4,6-disubstituted pyrimidine or a 3,6-disubstituted pyridazine.[16]

The work we report herein is aimed at the control of nano-mechanical features by the choice of the appropriate heterocyclic units. We describe the coordinative properties of ligands **2** and **4** (Scheme 4), consider the remarkable modifications caused by the simple replacement of a pym

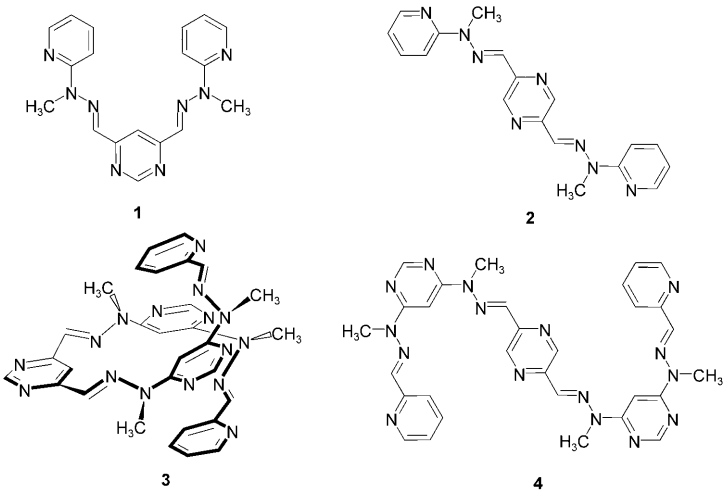

Scheme 4. Ligands py_1-hyz-pym-hyz-py_1 (**1**), py_1-hyz-pz-hyz-py_1 (**2**), py_1-(hyz-pym)$_3$-hyz-py_1 (**3**) and py_1-hyz-pym-hyz-pz-hyz-pym-hyz-py_1 (**4**).

group in **1** and **3**[10b] (Scheme 4) by a pz group in ligands **2** and **4**, and reflect on the implications of such a behaviour.

Results and Discussion

Ligand synthesis: Ligands **1**[10b] and **3**,[10b] as well as **2**,[13a] were obtained as previously described. Ligand **4** was synthesised (Scheme 5) in five steps starting from 4,6-dichloropyrimidine (**5**) and 2,5-dimethylpyrazine (**8**). The pyrimidine **5** is heated to reflux with methylhydrazine under argon to give the dihydrazine **6**, the reaction of which with 2-pyridinealdehyde leads to precursor **7**.[10b] Reaction of **8** with benzaldehyde and benzoic anhydride leads to the corresponding 2,5-distyrylpyrazine **9**,[17] the reaction of which with O_3 in MeOH, followed by reduction with an aqueous solution of sodium metabisulfite, gives the dialdehyde **10**.[18] Ligand **4** was synthesised by condensation of 2 equiv of precursor **7** with 1 equiv of dialdehyde **10** in EtOH (Scheme 5). It is a yellowish solid, insoluble in EtOH or MeCN, and it has a low solubility in $CHCl_3$ or $C_2H_2Cl_4$.

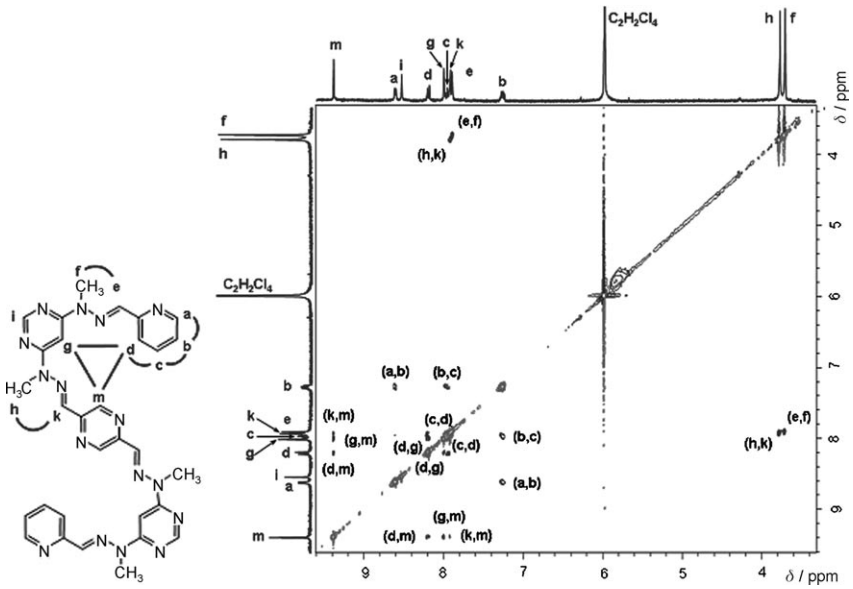

Figure 1. NOESY spectrum of ligand **4** ($C_2D_4Cl_2$, 300 MHz, 60 °C).

Conformation of ligand 4: 2D ^1H–^1H NOESY NMR spectroscopy was used to analyse the conformation of the free ligand **4** (Figure 1). The NOE correlations (f,e) and (h,k) between the CH_3 protons and the neighbouring −CH=N− imine proton confirm the conformation of the hyz groups. The correlation (d,g) between the C5 proton of pym (g) and the C3 proton of py_1 (d), as well as the correlation (g,m) between the C5 proton of pym (g) and the C3 (or C6) proton of pz (m) confirm the *transoid* conformations of the geometry codons (Figure 1). The low intensity (k,m) correlation id due to a weak interaction between protons k and m. The overall shape of the molecule of ligand strand **4** resembles the letter Z, as specified in the encoding functions of the pym and pz rings.

Formation of polynuclear linear metallo-supramolecular architectures by ligand 4 with Zn^{II} and Pb^{II}: Reaction of ligand **4** with 4 equiv of $Zn(OTf)_2$ (TfOH = triflic acid) in acetonitrile leads to the solubilisation of the ligand. The ^1H NMR spectrum contains sharp signals. The NOESY spectrum shows the NOEs (d,e) between the C3 proton of py_1 (d) and the −CH=N− proton (e), (f,g) and (g,h) between the CH_3 (f or h) and the C5 proton of pym (g), and (k,m) between the −CH=N− proton (k) and the C3 (or C6) protons of pz (m) (Figure 2). The NOEs (f,e) and (h,k) between the CH_3 protons and the neighbouring −CH=N− imine proton, present in the free ligand, are also observed and they confirm the conformation of the hyz groups. The observed NOEs are consistent with the extended structure corresponding to the tetranuclear linear architecture **4**-Zn_4 (= $[Zn_4(\mathbf{4})(OTf)_8]$) (Figure 2).

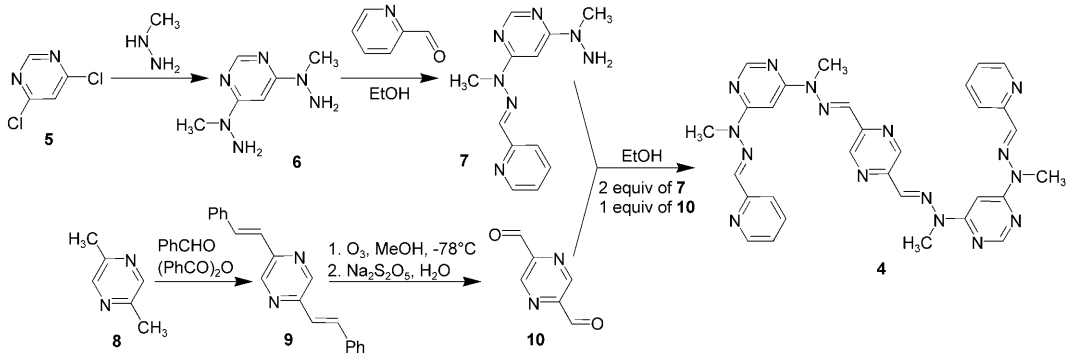

Scheme 5. Synthesis of ligand **4**.

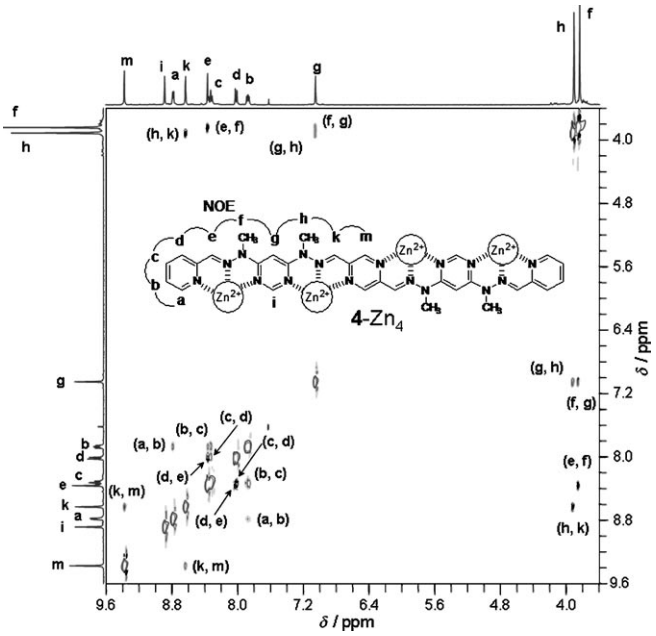

Figure 2. NOESY spectrum of the complex **4**-Zn_4 (=[Zn_4(**4**)$(OTf)_8$]) (CD_3CN, 300 MHz, 25 °C).

X-ray diffraction crystallography on single crystals of **4**-Zn_4 confirm the linear structure of the complex, with a length of about 31.1 Å. These data are consistent with the geometric principles presented above. The distance between the Zn^{II} ions separated by a pym unit (about 6.2 Å) is shorter than when they are separated by the central pz unit (about 7.1 Å). Coordination bonds and angles are listed in Table 1. Each Zn^{II} cation has an octahedral coordination sphere (Scheme 6d) constituted by the N_3 tridentate sequence (py1-hyz-pym or pym-hyz-pz), the O atoms from two water molecules and the N atom of an acetonitrile molecule ($N_{acetonitrile}$–Zn distances: 2.123 and 2.071 Å). The length and geometry of complex **4**-Zn_4 (Scheme 6d) may be compared with those of the tetranuclear Pb^{II} complex of ligand **3** (**3**-Pb_4[11b]; Scheme 6c). As expected, due to the larger size of Pb^{II}, complex **3**-Pb_4 is somewhat longer (about 32.2 Å) than **4**-Zn_4. Complex **3**-Pb_4 is slightly curved. In **4**-Zn_4 the two dinuclear curved moieties that contain the pym units are oriented in opposite directions, due to the replacement of the central pym unit of **3** by a pz unit in **4** that has an inversion centre. As a result, the metallic centres of **4**-Zn_4 are aligned in a quasi-linear array (Scheme 6d).

Model ligands 1, 2 and their complexes: A similar effect of the replacement of a pym unit by a pz unit is observed by comparing the dinuclear Pb^{II} complexes **1**-Pb_2 and **2**-Pb_2 (Scheme 6a,b). The Pb–Pb distance in the pz-based complex **2**-Pb_2 is longer (about 8.2 Å) than that in the pym-based one **1**-Pb_2 (about 6.9 Å), whereas the overall length of the complexes is in both cases about 18.1 Å.

Complex **2**-Pb_2 was obtained by reaction of ligand **2** with 2 equiv of $Pb(CF_3SO_3)_2$ in acetonitrile (for coordination bond lengths and angles, see Table 1). A coordination polymer is generated in the solid state (Figure 3).

Reversible extension/contraction molecular motions: pH-controllable supramolecular systems[19] performing nano-mechanical molecular motions[20] have received increasing attention. Thus, acid–base-controllable devices have been reported such as, for example, a bistable molecular muscle based on a doubly threaded Janus-type [2]rotaxane,[21] a resorcin[4]arene-based container,[22] phenanthroline-derived oligoamide foldamers[23] and a block-selective mobile polyrotaxane for displacement of cyclodextrins.[24]

Reversible extension/contraction motions of helical and linear ligand molecules, mediated by cation binding and release and fuelled by acid–base neutralisation, have been induced on sequential acid–base addition in the presence of a competing ligand.[11,12,25] Similar processes may be generated by using ligand **4** and its extension on interaction with Zn^{II} to give the corresponding complex **4**-Zn_4. A stronger ancillary ligand tris(2-aminoethyl)amine (tren)—the coordinating capacities of which are modulated by protonation—may interact with complex **4**-Zn_4 and abstract the Zn^{II} ions from **4**-Zn_4, thus regenerating the contracted ligand **4**. Subsequent alternate addition of acid and base will modulate the binding and release of Zn^{II} from its tren complex, and will generate the contraction/extension motions of strand **4**.

Indeed, the reversible formation of complex **4**-Zn_4 by extension of ligand **4** was followed by ^{1}H NMR spectroscopy (Figure 4). Ligand **4** has very poor solubility in CD_3CN, whereas the Zn^{II} complex is insoluble in $CDCl_3$ and no compromise mixture of these two solvents that is able to dissolve both ligand and complex has been found. The ^{1}H NMR spectrum of **4** was recorded in $CDCl_3$ (Figure 4, spectrum 1). After the evaporation of $CDCl_3$, the addition of CD_3CN followed by 4 equiv of $Zn(OTf)_2$ resulted in its solubilisation (Figure 4, spectrum 2). Addition of 4 equiv of a stronger ligand, tren, to this Zn^{II} complex removed the Zn^{II} cations from **4**-Zn_4 and restored the contracted form of the free ligand **4**. The spectrum was recorded in CD_3CN (Figure 4, spectrum 3) and then, after evaporation of CD_3CN, in $CDCl_3$ (Figure 4, spectrum 4). Subsequent addition of 12 equiv of TfOH in CD_3CN (Figure 4, spectrum 5) produced protonation of tren and release of Zn^{II}, thus resulting in the formation of the tetranuclear complex **4**-Zn_4. Finally, addition of the corresponding quantity of Et_3N resulted in deprotonation of tren that became able to bind the Zn^{II}

Table 1. Coordination bond lengths and angles in complexes **2**-Pb_2 and **4**-Zn_4.

Complex	M	N_{py}–M [Å]	N_{hyz}–M [Å]	N_{pym}–M [Å]	N_{pz}–M [Å]	M–M [Å]	N_{py}-M-N_{hyz} [°]	N_{hyz}-M-N_{pz} [°]	N_{hyz}-M-N_{pym} [°]
2-Pb_2	Pb	2.502	2.607	–	2.700	8.172	61.62	62.90	–
4-Zn_4	Zn	2.128	2.144	2.180	2.176	6.222	75.46	74.57	72.76
			2.133	2.117		7.131			73.58

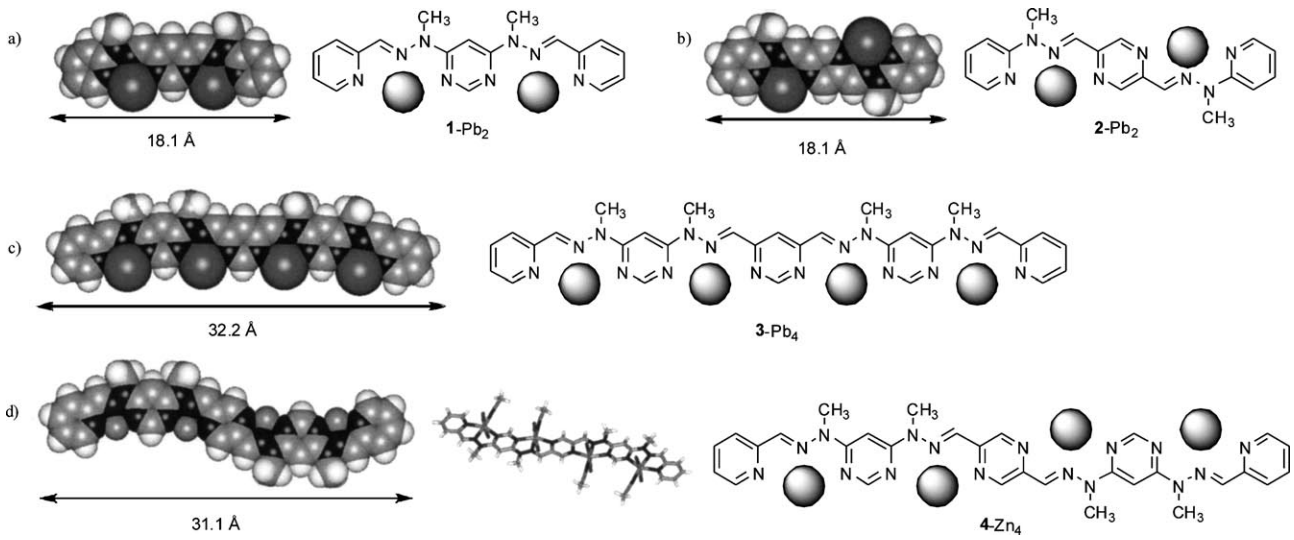

Scheme 6. X-ray molecular structure of the complexes **1**-Pb_2[11b] (a), **2**-Pb_2 (b), **3**-Pb_4[11b] (c) and **4**-Zn_4 (d) ($CF_3SO_3^-$ anions not shown).

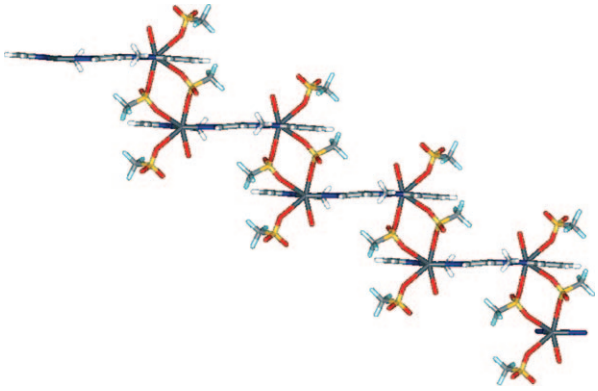

Figure 3. Coordination polymer in the crystal structure of complex **2**-Pb_2.

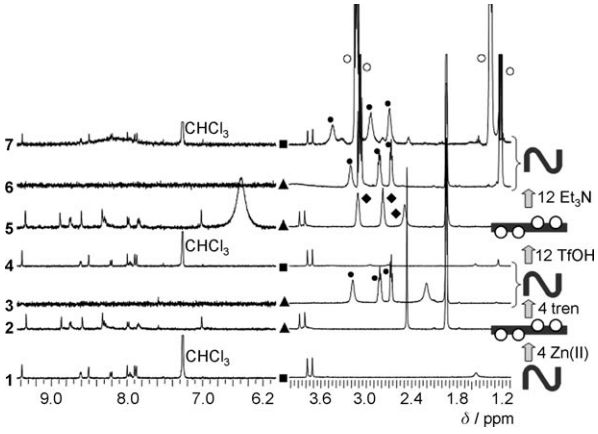

Figure 4. Reversible inter-conversion of ligand/complex generating extension/contraction molecular motions of ligand **4** (400 MHz). Solvents: ■ = $CDCl_3$, ▲ = CD_3CN. Other species: ● = $(trenH_3)^{3+}$, ◆ = $(Zn,tren)^{2+}$, ○ = Et_3NH^+. The aromatic domain (left) of the spectra is amplified by a factor of ≈4 with respect to the aliphatic region (right).

ions, thus regenerating the free contracted ligand **4** (Figure 4, spectra 6 and 7).

The length of ligand **4** is about 12 Å and that of the corresponding tetranuclear Zn^{II} complex is about 31 Å, which gives an amplitude of motion Δl_{pz} of 19 Å. On the other hand, the length of ligand **3** is about 4.5 Å and that of the corresponding tetranuclear Pb^{II} complex is about 32 Å (amplitude $\Delta l_{pym} = 28$ Å). The difference in amplitude $\Delta l_{pym} - \Delta l_{pz}$ between the molecular motions of ligands **4** and **3**, of about 9 Å, clearly shows the efficiency of length and geometry control by the choice of the central heterocycle.

Ru^{II} tetranuclear rack-like complex 4-[Ru(terpy)]$_4$: Reaction of ligand **4** with 5 equiv of $[Ru(terpy)]Cl_3$ in an EtOH/water 1:1 mixture at reflux during 20 h, followed by precipitation by anion exchange with NH_4PF_6, led to a green precipitate of the rack-like complex **4**-$[Ru(terpy)]_4$ (= $[Ru_4(\mathbf{4})(terpy_4)](PF_6)_8$). 1D and 2D NMR data confirmed its structure. Thus, ^1H–^1H NOESY allowed assignment of proton resonances and displayed the characteristic NOEs expected for the conformational changes due to Ru^{II} coordination, which induces the transformation of the all-*transoid* form into the all-*cisoid* one. The shape of the coordinated ligand is established by NOEs that do not exist in the free ligand but appear after coordination, such as (d,e), (f,g), (h,i) and (j,k) (Figure 5). The present four-site Ru^{II} rack **4**-$[Ru(terpy)]_4$ contains two dinuclear motifs analogous to those of previously reported dinuclear rack-like complexes.[13a]

The ^1H NMR spectrum of the complex **4**-$[Ru(terpy)]_4$ is to be compared with the spectra of complexes **1**-$[Ru(terpy)]_2$ and **2**-$[Ru(terpy)]_2$ (Figure 6). Complex **1**-$[Ru(terpy)]_2$ contains as a bridging ligand the bis-terpy-like ligand obtained by condensation of 4,6-bis(methylhydrazino)pyrimidine with 2 equiv of 2-pyridinecarboxaldehyde, whereas the bridging ligand of **2**-$[Ru(terpy)]_2$ is obtained by condensation of 2,5-pyrazinedicarboxaldehyde with 2 equiv of 2-methylhydrazinopyridine. The py_1-hyz-pym motif of **1**-

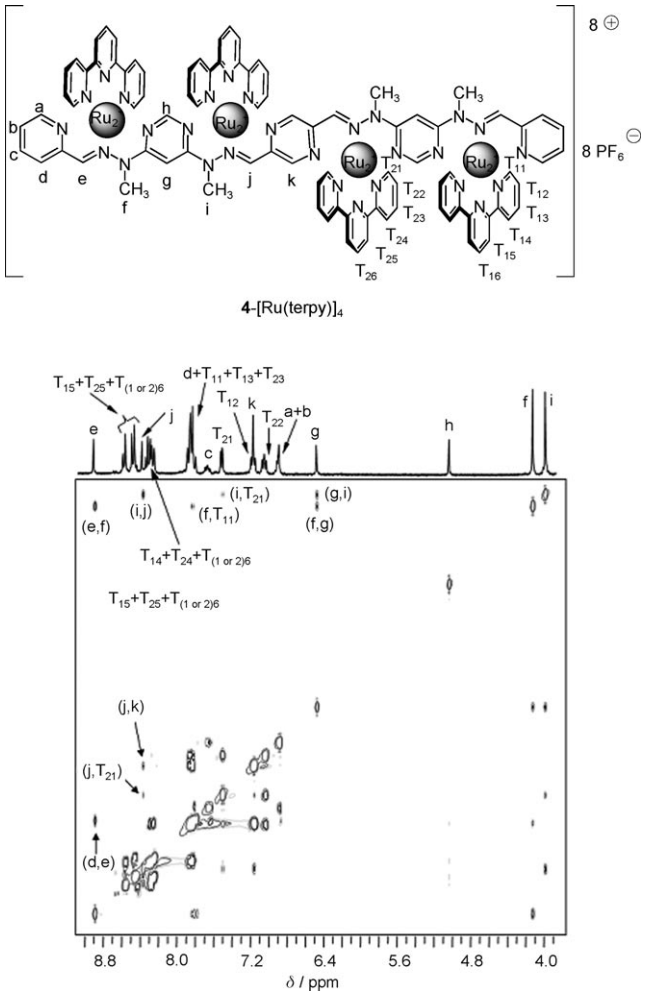

Figure 5. NOESY spectrum of the complex **4**-[Ru(terpy)]$_4$ (=[Ru$_4$(**4**)(terpy$_4$)](PF$_6$)$_8$) (CD$_3$CN, 300 MHz, 25 °C).

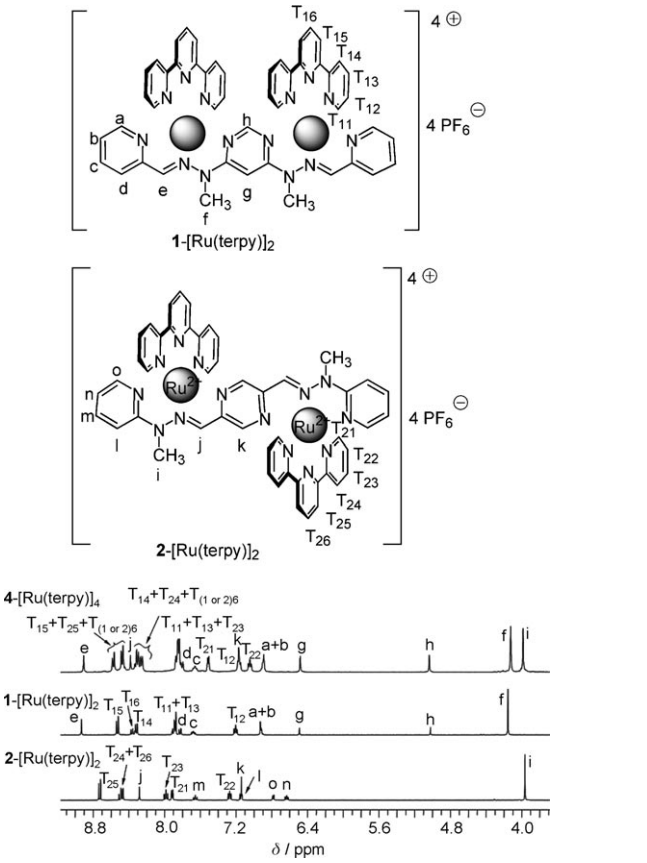

Figure 6. Comparison of the ^{1}H NMR (CD$_3$CN, 400 MHz) spectra of complexes **1**-[Ru(terpy)]$_2$,[13a] **2**-[Ru(terpy)]$_2$[13a] and **4**-[Ru(terpy)]$_4$.

[Ru(terpy)]$_2$ is contained in **4**-[Ru(terpy)]$_4$ and the chemical shifts of protons a–h are close in the two complexes. Similarly, the hyz-pz-hyz motif of **2**-[Ru(terpy)]$_2$ is contained in **4**-[Ru(terpy)]$_4$ (protons i–k).

Dependence of the shape of the ligand strand and of the amplitude and relative direction of the molecular motions on the nature of the heterocycles: As pointed out above, the global shape of a hyz-based strand can be controlled by the choice and combination of the heterocyclic units pym and pz. Thus, (pym-hyz)$_n$ strands present helical folding, (pz-hyz)$_n$ ones are linear and (pym-hyz-pz-hyz)$_n$ strands are of undulating zigzag type (Scheme 7, Table 2).

The above structural principles led us to the design of the present new class of hyz-based ligands, which incorporate both pym and pz heterocycles, to control both the molecular shape and amplitude of the extension/contraction motions. The starting system was the ligand py$_1$-(hyz-pym)$_3$-hyz-py$_1$ (**3**) that reacts with Pb^{II} to give a tetranuclear stick-like complex **3**-Pb$_4$ (=[Pb$_4$(**3**)(OTf)$_8$]), in which the length of the unfolded ligand is about 32 Å.

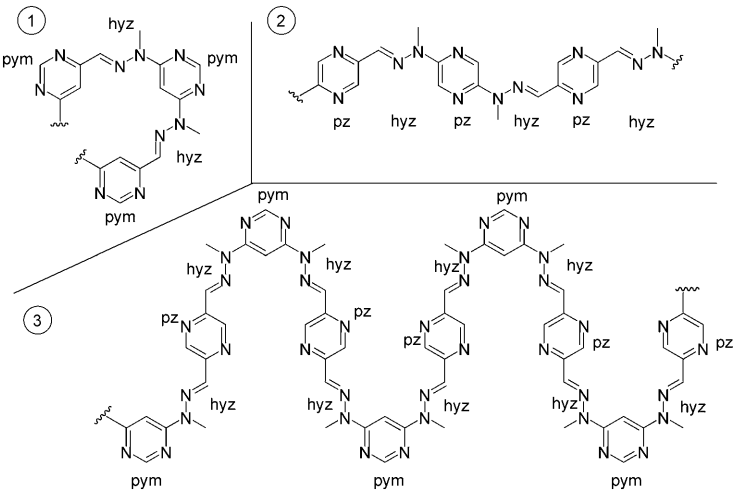

Scheme 7. Control of strand shape by choice of the heterocyclic units: 1) helical (pym-hyz)$_n$; 2) linear (pz-hyz)$_n$; 3) undulating (pym-hyz-pz-hyz)$_n$.

As the free, uncoordinating hyz-pz unit encodes linear shape, the replacement of the central pym of **3** by a pz unit introduced a linear part, thus increasing the distance between the N atoms of the two terminal py units from 6.9 Å

Table 2. Control of strand shape and motion amplitude by the nature of the heterocyclic units.

Sequence	Strand shape	Complex shape	Amplitude
$(pym\text{-}hyz)_n$	helical	linear ("*syn*")	large
$(pz\text{-}hyz)_n$	linear	linear ("*anti*")	small
$(pz\text{-}hyz\text{-}pym\text{-}hyz)_n$	undulating	linear	intermediate

(ligand strand **3**) to 18.6 Å (ligand strand **4**). On the other hand, both hyz-pym and hyz-pz act as linearity codons on coordination, and consequently the replacement of the central pym (ligand **3**) by a pz unit (ligand **4**) led to a stick-like tetranuclear complex **4**-Zn_4 having globally a length very close to that of its pym analogue **3**-Pb_4.

The lengths of stick-like tetranuclear complexes of ligands **3** and **4** are similar ($l_3 \approx l_4$), although the lengths of the free ligands are different ($l_1 \neq l_2$). It thus becomes possible to change the motional amplitude by changing the central unit. The two amplitudes may be defined as $\Delta l_{pym} = l_3 - l_1$ and $\Delta l_{pz} = l_4 - l_2$. But l_3 and l_4 being almost equal, the amplitude depends only on the length of the free ligands, l_1 and l_2, which itself depends on the nature of the central heterocycle (Figure 7).

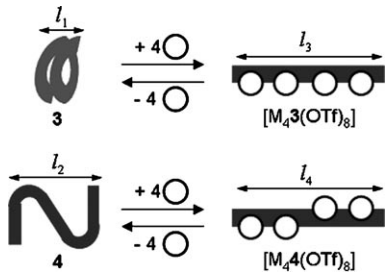

Figure 7. Control of the amplitude of motion on cation coordination, depending on the nature of the central ring: pym for **3** and pz for **4**.

One may also note that ligand **4**, which combines pym and pz groups, contains local domains that will behave, in terms of relative displacements, either in the *syn* or *anti* fashion, as in the model ligands **1** and **2** (see also Scheme 3). Ligand **4** thus illustrates the ability to control both the local shape and local motion through appropriate selection of the heterocyclic components.

Conclusion

The present results demonstrate the possibility of enforcing the global shape of a molecular ligand strand (folded helix versus undulating zigzag) by selecting and combining appropriate heterocyclic units. Furthermore, the grafting of given het-hyz sequences on a central core heterocyclic unit allows the control of both the amplitude and especially of the relative direction of the motions generated on metal-ion binding. In particular, the replacement of a central 4,6-disubstituted pyrimidine by a 2,5-disubstituted pyrazine produces a decrease of the amplitude of the subsequent molecular motions, as well as a change in the nature of relative motions of the branches connected to these rings, from "flapping"-type (*dis*-sense) motions (pym) to "twirling"-type (*con*-sense) motions (pz). The combination within ligands of different encoding units allows the generation of hybrid strand folding as well as of combined molecular motions.

Experimental Section

Materials and general methods: The following compounds were prepared as previously described: **1**,[10b] **2**,[13a] **3**,[10b] **6**,[10b] **7**,[10b] **9**,[17] **10**,[18] **1**-Pb_2,[11b] **3**-Pb_4,[11b] **1**-$[Ru(terpy)]_2$,[13a] **2**-$[Ru(terpy)]_2$,[13a] and $[Ru(terpy)]Cl_3$.[26] The following reagents were purchased from commercial sources: $RuCl_3$ (Aldrich, Avocado), terpy (Aldrich, Avocado), 2,5-dimethylpyrazine (Aldrich), benzaldehyde (Aldrich), and benzoic anhydride (Aldrich). 400 MHz ^{1}H NMR spectra were recorded on a Bruker Ultrashield Avance 400 spectrometer and 300 MHz ^{1}H NMR spectra were recorded on a Bruker 300 spectrometer. The solvent residual signal was used as an internal reference for ^{1}H NMR spectra ($CHCl_3$ $\delta = 7.26$ ppm, CH_3CN $\delta = 1.94$ ppm). The following notation is used for the ^{1}H NMR spectral splitting patterns: singlet (s), doublet (d), triplet (t), multiplet (m). The 2D-NMR experiments employed were COSY (correlation spectroscopy) and NOESY (nuclear Overhauser enhancement spectroscopy or nuclear Overhauser and exchange spectroscopy); they were carried out on 300 MHz Bruker spectrometers. ESIMS measurements were performed by the Service de Spectrométrie de Masse, Université de Strasbourg.

CCDC-743475 (**2**-Pb_2) and 743476 (**4**-Zn_4) contain the supplementary crystallographic data for this paper. These data can be obtained free of charge from the Cambridge Crystallographic Data Centre via www.ccdc.cam.ac.uk/data_request/cif.

Ligand and complex synthesis and characterisation

4: A solution of **10** (114.1 mg, 0.84 mmol) and **7** (436 mg, 1.7 mmol) in CH_2Cl_2 (25 mL) and EtOH (10 mL) was stirred at 36 °C during 6 h. The yellow solid that precipitated was separated by centrifugation, washed with CH_2Cl_2 and dried under vacuum to yield **4** (431 mg, 83 %). ^{1}H NMR ($CDCl_3$, 400 MHz, reference: solvent residual peak, $\delta = 7.26$ ppm): $\delta =$ 9.39 (s, 2H; H_m), 8.63–8.59 (m, 2H; H_a), 8.50 (s, 2H; H_i), 8.20 (d, $J =$ 8.8 Hz, 2H; H_d), 7.99 (s, 2H; H_g), 7.99–7.91 (m, 2H; H_c), 7.90 (s, 2H; H_k), 7.87 (s, 2H; H_e), 3.78 (s, 6H; H_h), 3.71 ppm (s, 6H; H_f); H_b is hidden by the residual $CHCl_3$ peak. The solubility of this ligand in $CDCl_3$ is too low to allow NOESY, so $C_2Cl_4D_2$ was used for this purpose, heated at 60 °C. HR-ESIMS: *m*/*z*: calcd for $[C_{30}H_{30}N_{16}+Li]^+$: 621.299 $[M+Li]^+$; found: 621.306.

2-Pb_2: $Pb(CF_3SO_3)_2$ (4 mg, 2.2 equiv) in CD_3CN (0.4 mL) was added to a suspension of ligand **2** (1.26 mg, 1 equiv) in CD_3CN (0.4 mL). ^{1}H NMR (CD_3CN, 400 MHz, reference: solvent residual peak, $\delta = 1.94$ ppm): $\delta =$ 9.31 (s, 2H; H_k), 8.61 (s, 2H; H_j), 8.58 (d, $J = 4.9$ Hz, 2H; H_o), 8.12–8.04 (m, 2H; H_m), 7.55 (d, $J = 8.8$ Hz, 2H; H_l), 7.40–7.35 (m, 2H; H_n), 3.75 ppm (s, 6H; H_i). After about 5 min, the complex crystallised out of the solution. Crystal data for **2**-Pb_2: formula $C_{26}H_{28}F_{12}N_{10}O_{14}Pb_2S_4$; formula weight: 1475.19; triclinic; space group: $P\bar{1}$ (No. 2); $a = 9.7810(1)$, $b = 11.2120(1)$, $c = 11.9373(2)$ Å; $\alpha = 63.140(5)$, $\beta = 82.711(5)$, $\gamma =$ 70.578(5)°; $V = 1100.98(7)$ Å^3; $Z = 1$; $\rho_{calcd} = 2.219$ g cm^{-3}; $\mu(Mo_{K\alpha}) =$ 7.949 mm^{-1}; $F(000) = 698$; $T = 173$ K; radiation $Mo_{K\alpha} = 0.71073$ Å; $2.5° \leq \theta \leq 30.0°$; dataset *hkl*: −13, 13; −15, 15; −15, 16; total unique data, *R*-(int) = 10331, 6397, 0.030; observed data with $[I > 2\sigma(I)]$: 5785; N_{ref}, $N_{par} = 5785$, 307; $R = 0.0210$, $wR2 = 0.0330$, $S = 1.05$; GOF = 1.055; min. and max. residual density = −0.23, 0.82 e A^{-3}.

4-Zn_4: Ligand **4** (1.9 mg, 3.1 μmol, 1 equiv) and $Zn(CF_3SO_3)_2$ (4.5 mg, 12.4 μmol, 4 equiv) were mixed with CD_3CN (0.6 mL) until dissolution. ^{1}H NMR (CD_3CN, 400 MHz, reference: solvent residual peak, $\delta =$ 1.94 ppm): $\delta = 9.33$ (s, 2H), 8.85 (s, 2H), 8.74 (d, $J = 5.0$ Hz, 2H), 8.59 (s, 2H), 8.32 (s, 2H), 8.29 (td, $J = 7.8$, 1.0 Hz, 2H), 7.98 (d, $J = 7.8$ Hz, 2H), 7.84 (dd, $J = 7.8$, 5.0 Hz, 2H), 7.01 (s, 2H), 3.88 (s, 6H), 3.81 ppm (s, 6H);

HR-ESIMS: *m/z*: calcd for $[Zn_4C_{36}H_{30}F_{18}N_{16}O_{18}S_6]^{2+}$: 884.552 (100%) $[M\text{-}2CF_3SO_3]^{2+}$; found: 884.848. Crystal data for **4**-Zn_4: formula $C_{38}H_{42}N_{20}O_8Zn_4{\cdot}4CF_3SO_3{\cdot}2CH_3CN$; formula weight: 1846.78; monoclinic; space group *C*2/*c* (No. 15); $a=22.2488(6)$, $b=19.7793(8)$, $c=22.5706(8)$ Å; $\alpha=90$, $\beta=91.333(2)$, $\gamma=90°$; $V=9929.9(6)$ Å^3; $Z=4$; $\rho_{calcd}=1.235$ g cm^{-3}; $\mu(Mo_{K\alpha})=1.121$ mm^{-1}; $F(000)=3720$; $T=173$ K; radiation $Mo_{K\alpha}=0.71073$ Å; $1.4° \le \theta \le 30.1°$; dataset *hkl*: −27, 31; −25, 27; −22, 31; total unique data, $R(int)=34455$, 14418, 0.067; observed data $[I>2\sigma(I)]=5404$; N_{ref}, $N_{par}=14418$, 384; $R=0.1211$, $wR2=0.3661$, $S=0.99$; GOF = 0.992; min. and max. residual density = −2.10, 4.19 e A^{-3}.

$[Ru_4(4)(terpy)_4](PF_6)_8$ (4-[Ru(terpy)]$_4$): Ethanol/water (5 mL, 1:1 v/v) was added to [Ru(terpy)]Cl_3 (26 mg, 0.059 mmol, 5 equiv) and ligand **4** (7.2 mg, 0.012 mmol, 1 equiv). The mixture was heated at reflux (heating bath temperature ≈115 °C) for 20 h, then cooled to room temperature and filtered. Excess aqueous NH_4PF_6 was added to the solution and the precipitate was collected. The solid was purified by re-precipitation from acetonitrile/$CHCl_3$ to afford **4**-[Ru(terpy)]$_4$ (12 mg, ≈33%) as a green solid. M.p. > 300 °C; ^{1}H NMR (CD_3CN, 300 MHz, reference: solvent residual peak, $\delta=1.94$ ppm): $\delta=8.91$ (s, 2H; H_e), 8.57 (d, $J=7.4$ Hz, 4H; H_{T15} or H_{T25}), 8.50–8.42 (m, 6H; H_{T15} or $H_{T25}+H_{T16}$ or H_{T26}), 8.38 (s, 2H; H_j), 8.35–8.22 (m, 10H; $H_{T14}+H_{T24}+H_{T16}$ or H_{T26}), 7.90–7.78 (m, 12H; $H_{T11}+H_{T13}+H_{T23}+H_d$), 7.69–7.62 (m, 2H; H_c), 7.53–7.48 (m, 4H; H_{21}), 7.20–7.14 (m, 6H; $H_{T12}+H_k$), 7.08–7.01 (m, 4H; H_{T22}), 6.92–6.86 (m, 4H; H_a+H_b), 6.48 (s, 2H; H_g), 5.04 (s, 2H; H_h), 4.12 (s, 6H; H_f), 3.98 ppm (s, 2H; H_l); HR-ESIMS: *m/z*: calcd for $[C_{30}H_{30}N_{16}{\cdot}4C_{15}H_{11}N_3{\cdot}4Ru{\cdot}6PF_6]^{2+}$: 1411.036 $[M-2PF_6]^{2+}$, found: 1411.024; *m/z*: calcd for $[C_{30}H_{30}N_{16}{\cdot}4C_{15}H_{11}N_3{\cdot}4Ru{\cdot}5PF_6]^{3+}$: 892.702 $[M-3PF_6]^{3+}$; found: 892.694.

Acknowledgements

We thank Dr. Lydia Brelot and Dr. André de Cian for recording the data and solving the X-ray structure of complexes **2**-Pb_2 and **4**-Zn_4. We thank Patrick Wehrung, Dr. Raymonde Baltenweck-Guyot and Romain Carrière for mass spectrometry analyses.

[1] For the protein folding, see: a) special issue on protein folding: *Acc. Chem. Res.* **1998**, *31*, 697–780, edited by J. R. Winkler, H. B. Gray; b) C. Branden, J. Tooze, *Introduction to Protein Structure*, Garland, New York, **1991**.

[2] For use of structural codons to induce linearity/helicity by pyridine/pyrimidine replacement in molecular strands, see: I. Odriozola, N. Kyritsakas, J.-M. Lehn, *Chem. Commun.* **2004**, 62–63.

[3] a) G. S. Hanan, J.-M. Lehn, N. Kyritsakas, J. Fischer, *J. Chem. Soc. Chem. Commun.* **1995**, 765–766; b) D. M. Bassani, J.-M. Lehn, G. Baum, D. Fenske, *Angew. Chem.* **1997**, *109*, 1931–1933; *Angew. Chem. Int. Ed. Engl.* **1997**, *36*, 1845–1847.

[4] M. Ohkita, J.-M. Lehn, G. Baum, D. Fenske, *Chem. Eur. J.* **1999**, *5*, 3471–3481.

[5] a) S. H. Gellman, *Acc. Chem. Res.* **1998**, *31*, 173–180; b) D. J. Hill, M. J. Mio, R. B. Prince, T. S. Hughes, J. S. Moore, *Chem. Rev.* **2001**, *101*, 3893–4012; c) I. Huc; S. Hecht, *Foldamers: Structure, Properties and Applications*, Wiley, New York, **2007**; d) C. M. Goodman, S. Choi, S. Shandler, W. F. DeGrado, *Nat. Chem. Biol.* **2007**, *3*, 252–262; e) K. D. Stigers, M. J. Soth, J. S. Nowick, *Curr. Opin. Chem. Biol.* **1999**, *3*, 714–723. For helicity induction in synthetic helical strands, see for instance: f) R. B. Prince, L. Brunsveld, E. W. Meijer, J. S. Moore, *Angew. Chem.* **2000**, *112*, 234; *Angew. Chem. Int. Ed.* **2000**, *39*, 228; g) T. Sanji, N. Kato, M. Kato, M. Tanaka, *Angew. Chem.* **2005**, *117*, 7467; *Angew. Chem. Int. Ed.* **2005**, *44*, 7301; h) C. Dolain, H. Jiang, J.-M. Léger, P. Guionneau, I. Huc, *J. Am. Chem. Soc.* **2005**, *127*, 12 943; i) M. Melucci, G. Barbarella, M. Gazzano, M. Cavallini, F. Biscarini, A. Bongini, F. Piccinelli, M. Monari, M. Bandini, A. Umani-Ronchi, P. Biscarini, *Chem. Eur. J.* **2006**, *12*, 7304; j) M. Waki, H. Abe, M. Inouye, *Chem. Eur. J.* **2006**, *12*, 7839; k) T. Sanji, N. Kato, M. Tanaka, *Org. Lett.* **2006**, *8*, 235.

[6] a) B. Gong, *Chem. Eur. J.* **2001**, *7*, 4336–4342; b) V. Berl, I. Huc, R. Khoury, J.-M. Lehn, *Chem. Eur. J.* **2001**, *7*, 2798; c) V. Berl, I. Huc, R. Khoury, J.-M. Lehn, *Chem. Eur. J.* **2001**, *7*, 2810.

[7] D. J. Hill, J. S. Moore, *Proc. Natl. Acad. Sci. USA* **2002**, *99*, 5053.

[8] a) K. T. Potts, K. A. Gheysen, Raiford, M. Keshavarz-K, *J. Am. Chem. Soc.* **1993**, *115*, 2793; b) For the role of linear codons of (hyzpy) units, see: A.-M. Stadler, N. Kyritsakas, J.-M. Lehn, *Chem. Commun.* **2004**, 2024–2025.

[9] a) S. T. Howard, *J. Am. Chem. Soc.* **1996**, *118*, 10269–10274; b) A. Göller, U.-W. Grummt, *Chem. Phys. Lett.* **2000**, *321*, 399–405; c) G. Corongiu, P. Nava, *Int. J. Quantum Chem.* **2003**, *93*, 395–404; d) G. Corongiu, P. Nava, unpublished ab initio computations; e) E. Ruiz, J.-M. Lehn, unpublished ab initio computations.

[10] a) K. M. Gardinier, R. G. Khoury, J.-M. Lehn, *Chem. Eur. J.* **2000**, *6*, 4124–4131; b) J.-L. Schmitt, A.-M. Stadler, N. Kyritsakas, J.-M. Lehn, *Helv. Chim. Acta* **2003**, *86*, 1598–1624.

[11] a) M. Barboiu, J.-M. Lehn, *Proc. Natl. Acad. Sci. USA* **2002**, *99*, 5201–5206; b) A.-M. Stadler, N. Kyritsakas, R. Graff, J.-M. Lehn, *Chem. Eur. J.* **2006**, *12*, 4503–4522.

[12] A.-M. Stadler, N. Kyritsakas, J.-M. Lehn, *Chem. Commun.* **2004**, 2024–2025.

[13] a) A.-M. Stadler, F. Puntoriero, S. Campagna, N. Kyritsakas, R. Welter, J.-M. Lehn, *Chem. Eur. J.* **2005**, *11*, 3997–4009; b) see also: J. Ramírez, A.-M. Stadler, G. Rogez, M. Drillon, J.-M. Lehn, *Inorg. Chem.* **2009**, *48*, 2456.

[14] F. Loiseau, F. Nastasi, A.-M. Stadler, S. Campagna, J.-M. Lehn, *Angew. Chem.* **2007**, *119*, 6256–6259; *Angew. Chem. Int. Ed.* **2007**, *46*, 6144–6147.

[15] J. Hausmann, S. Brooker, *Chem. Commun.* **2004**, 1530–1531.

[16] B. R. Manzano, F. A. Jalón, I. M. Ortiz, M. L. Soriano, F. Gómez de La Torre, J. Elguero, M. A. Maestro, K. Mereiter, T. D. W. Claridge, *Inorg. Chem.* **2008**, *47*, 413–428.

[17] M. Hasegawa, Y. Asusuki, F. Susuki, H. Nakanishi, *J. Polym. Sci. A-1* **1969**, *7*, 743–752.

[18] a) R. H. Wiley, *J. Macromol. Sci. Chem. A* **1987**, *24*, 1183; b) R. H. Wiley, U.S. Patent, 4260757, **1981**.

[19] For a review, see: K. C.-F. Leung, C.-P. Chak, C.-M. Lo, W.-Y. Wong, S. Xuan, C. H. K Cheng, *Chem. Asian J.* **2009**, *4*, 364–381.

[20] For reviews, see: a) R. P. Feynman, *Eng. Sci.* **1960**, *23*, 22–36; b) A. P. Davis, *Nature* **1999**, *401*, 120–121; c) V. Balzani, A. Credi, F. M. Raymo, J. F. Stoddart, *Angew. Chem.* **2000**, *112*, 3484–3530; *Angew. Chem. Int. Ed.* **2000**, *39*, 3348–3391; d) B. L. Feringa, *Nature* **2000**, *408*, 151–154; e) special issue on molecular machines: *Acc. Chem. Res.* **2001**, *34*, 409–522; f) special issue on molecular machines and motors: *Struct. Bonding* **2001**, *99*, 1–281; g) V. Balzani, A. Credi, M. Venturi, *Chem. Eur. J.* **2002**, *8*, 5524–5532; h) V. Balzani, M. Venturi, A. Credi, *Molecular Devices and Machines: A Journey into the Nanoworld*, Wiley-VCH, Weinheim, **2003**; i) C. J. Easton, S. F. Lincoln, L. Barr, H. Onagi, *Chem. Eur. J.* **2004**, *10*, 3120–3128; j) C. P. Mandl, B. König, *Angew. Chem.* **2004**, *116*, 1650–1652; *Angew. Chem. Int. Ed.* **2004**, *43*, 1622–1624; k) G. S. Kottas, L. I. Clarke, D. Horinek, J. Michl, *Chem. Rev.* **2005**, *105*, 1281–1376; l) K. Kinbara, T. Aida, *Chem. Rev.* **2005**, *105*, 1377–1400; m) E. R. Kay, D. A. Leigh in *Functional Artificial Receptors* (Eds.: T. Schrader, A. D. Hamilton), Wiley-VCH, Weinheim, **2005**, pp. 333–406; n) *Top. Curr. Chem.* **2005**, *262*, 1–236; o) special issue on molecular motors: *J. Phys.: Condens. Matter* **2005**, *17*, S3661–S4024; p) D. A. Leigh, F. Zerbetto, E. R. Kay, *Angew. Chem.* **2007**, *119*, 72–196; *Angew. Chem. Int. Ed.* **2007**, *46*, 72–191.

[21] J. Wu, K. C.-F. Leung, D. Benitez, J.-Y. Han, S. J. Cantrill, L. Fang, J. F. Stoddart, *Angew. Chem.* **2008**, *120*, 7580–7584; *Angew. Chem. Int. Ed.* **2008**, *47*, 7470–7474.

[22] a) T. Gottschalk, P. D. Jarowski, F. Diederich, *Tetrahedron* **2008**, *64*, 8307–8317; b) V. A. Azov, A. Schlegel, F. Diederich, *Angew. Chem.* **2005**, *117*, 4711–4715; *Angew. Chem. Int. Ed.* **2005**, *44*, 4635–4638.

[23] H.-Y. Hu, J.-F. Xiang, Y. Yang, C.-F. Chen, *Org. Lett.* **2008**, *10*, 1275–1278.

[24] H. S. Choi, A. Hirasawa, T. Ooya, D. Kajihara, T. Hohsaka, N. Yui, *ChemPhysChem* **2006**, *7*, 1671–1673.

[25] a) M. Barboiu, G. Vaughan, N. Kyritsakas, J.-M. Lehn, *Chem. Eur. J.* **2003**, *9*, 763–769; b) A.-M. Stadler, N. Kyritsakas, G. Vaughan, J.-M. Lehn, *Chem. Eur. J.* **2007**, *13*, 59–68; c) J. Ramirez, A.-M. Stadler, L. Brelot, J.-M. Lehn, *Tetrahedron* **2008**, *64*, 8402–8410.

[26] B. P. Sullivan, J. M. Calvert, T. J. Meyer, *Inorg. Chem.* **1980**, *19*, 1404.

Received: October 6, 2009
Published online: April 1, 2010

